

Mechanical characterization of membrane like microelectronic components

M. Držik^a, H. Löschner^b, E. Haugeneder^b, W. Fallman^c, P. Hudek^d, I.W. Rangelow^e, Y. Sarov^e, T. Lalinsky^f, J. Chlipak^a

Micromachined thin membranes are often used as basic structural elements of MEMS but in recent years extensive research has been done also on the application of large membranes as stencil mask. Such masks are necessary for ion or electron beam projection lithography where the patterns are formed as openings in a membrane. Both the overall shape and pattern distortions of the membrane can be caused by the materials used, the fabrication process, specific structure of the membrane, clamping forces in the aligner or by intrinsic stress state. Among the properties which has to be usually analysed are mechanical stresses, stress stability, thermal conductivity, vibration modes structure and flatness as well as thickness variations.

To enhance diagnostic capability for membranes methods based on optical principles were elaborated. Main advantage of the laser-based metrology is its contactless and non-destructive nature, thus even tiny membrane structures can be inspected.

Bulging method of membrane tension evaluation

Bulge testing was one of the first techniques to study membrane tension stress. During the test a uniform load pressure is applied to one face of the membrane properly clamped or supported over its edge and the induced membrane deformation is then measured. The method is commonly used for the determination of mechanical characteristics of membranes, however it is known that several problems and limitations are related to the interpretation of the results obtained.

The bulging method for stress measurement makes use of second order differential equilibrium equation

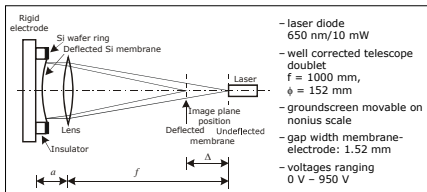
$$\frac{\partial^2 w}{\partial x^2} + \frac{\partial^2 w}{\partial y^2} = -\frac{p}{T} \quad \frac{1}{R_x} + \frac{1}{R_y} = -\frac{p}{T}$$

x, y – the coordinates of the point of the membrane surface, p – the acting pressure, T – the tension force per unit length. The second order derivatives can be expressed by the principal radii of curvature R_x, R_y with respect to the orthogonal coordinates. There are several assumptions for this formula:

- The thickness of the membrane is uniform
- Membrane has no openings
- Elasticity constants are uniform and isotropic
- The pressure is constant and isotropic
- Boundary conditions are compatible with the membrane deformation

Radii of curvature are measured experimentally.

The best solution – direct radii of curvature autocollimation focus shift measurement



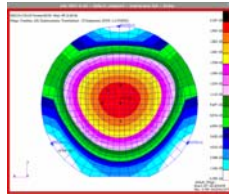
At the optical scheme the mirror-like membrane surface acts as a spherical mirror. Shift of the focal plane position due to spherical deformation of the membrane is expressed by a simple ray tracing

$$R_{x,y} = 2 \left(\frac{f^2}{\Delta} + f^2 - a \right)$$

Attractions of focus shift measurement

- straightforward determination of radii of curvature
- monitoring of any deviation from sphericity of membrane surface
- integral gathering of whole membrane surface information
- sensitivity of deformation measurement comparable with that of interferometrically obtained
- simple to arrange in optical laboratory

Excellent real achieved precision of membrane stress measurement $\Delta\sigma = \pm 0.1$ MPa.



- Deformation of the mask due to gravity in z-direction, mask is supported at the outer boundary of the wafer ring at 90°, 210° and 330°. Initial prestress is 1.7 MPa.

For actual calculation it has to be distinguished between the intrinsic prestress of the membrane and the stress induced by bulging force

$$\sigma_0 + \sigma_p = -\frac{pR}{2d}$$

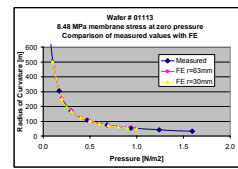
σ_0, σ_p – tensile stresses related to the force T , d – membrane thickness, R – mean change of membrane radius of curvature, σ_p – added membrane stress

$$\sigma_p = \frac{E}{1-\nu} \frac{r^2}{6R^2}$$

σ_0 – internal stress which has to be determined, r – half diameter of the circular membrane.

An electrical pressure between the membrane and a second electrode and different electrical potential U was used to deflect the membrane

$$p = \frac{1}{2} \epsilon_0 \epsilon_r U^2$$



- Radius of curvature of the equivalent sphere versus applied pressure, comparison of the measured values with FE analyses

Whole field large membrane thickness variations measurement

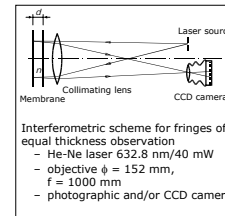
One of the key points of membrane mechanical characterization is also the measurement of its thickness variations throughout the area. The thickness is usually several microns, typically 3 μm

The membrane is an element similar to that of thin planparallel plate. The silicon transparency is enough to pass the light through the membrane thickness even in the visible red light.

The light intensity in the interference field of two beams is expressed by the following equation:

$$I = I_1 + I_2 + 2\sqrt{I_1 I_2} \cos\left(\frac{4\pi}{\lambda} nd - \pi\right)$$

I_1, I_2 – the intensities of the beams reflected from the front and the rear side of the membrane, respectively, λ – the light wavelength, n – the membrane index of refraction, d – the membrane thickness.



Contrast of the interference fringes:

$$\eta = 2 \frac{1-R'}{1+(1-R')^2} \quad R' = \left(\frac{n-1}{n+1} \right)^2$$

R' – reflectivity of the membrane surfaces, n – index of refraction of membrane material (Si)

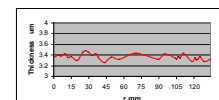
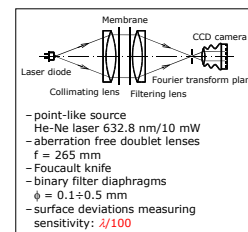
Index of refraction of Si:
 $n = 3.89$ (He-Ne laser, 632.8 nm)
 $\eta = 91\%$ (without absorption)

The main advantage of such a scheme realization – stability and high sensitivity.

Fringe value (the thickness change between two neighboring fringes): $C = 81$ nm

The sensitivity can be increased by numerical image processing (interpolation) up to several nm.

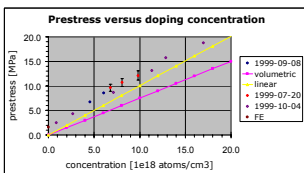
Besides using of interferometry also the classic optical shadow or phase visualization techniques can be realized. To obtain the topology of thick membrane scheme of optical filtering has been arranged.



- Thickness profile transversally through the membrane diameter

Stress vs. Boron doping relationship In-situ stress evaluation

In order to stay flat, the thin membrane must have tensile stress. To adjust the proper tensioning the fabrication process includes a step where Boron doping induces tension. Establishing proper process parameters a measurement of the stress in unstructured membranes vs. doping concentration is necessary. Due to its importance there were many works dedicated to the quantitative measurement of this relationship. Determination of membrane tension offers a chance to define this dependence very precise.



- Initial membrane prestress versus doping concentration of Boron, different measured stresses are compared with analytical calculations (Butschke, ims chips) and the FE calculation of the membrane stress according to a 1.7 MPa initial membrane layer stress on the SOI wafer (measured at ims chips)

Each experimental value represents the mean value of stress of several individual measurements at different pressure loads. The total error of the measurement has been calculated according to the rules of Gaussian error distribution. The error of the measured data is considered as statistical. The contributions are added quadratically. The error of constants of the apparatus which are needed for the calculation, are systematic and are summed.

Carbon/DLC layers are attractive materials for various applications in microelectronics. One of their perspective role – protective layers for ion beam lithographic masks (minireticles)

A study on the influence of ion bombardment by He⁺ and Ar⁺, respectively, on both the thickness and the internal membrane stress of C-layer has been performed.

In carbon film the ion irradiation causes expressive microstructural changes (due to variety of carbon modifications). They are followed by in-plane strains, and consequently, affect overall membrane stress.

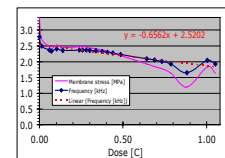
After irradiation c-film is strongly attacked by ambient air components → in-situ stress state had to be measured.

Irradiation inside vacuum chamber

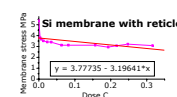
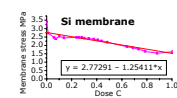
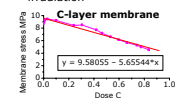
- Square-shaped 10x10 mm²/3 μm thick carbon covered Si membranes
- He⁺ – impact energy 10 keV, average current density 4.13 μA/cm²
- Ar⁺ – impact energy 5 keV, current density 13.3 μA/cm²



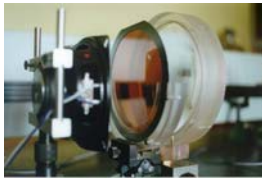
- Membrane stress evaluation
 - resonant frequency measurement inside vacuum,
 - electrostatic excitation
- Measurement of the first natural mode frequency
 - photoelectrical detection through the glass window autofocus detector adapted for inside vacuum use
- Mode shapes identification
 - by shadow visualization



- The membrane stress evolution of Si membrane covered by carbon layer after Ar⁺ irradiation



Membrane stress evaluation by resonant frequency method



Resonant frequencies of the membrane are tightly related to its tensile stress. The task to measure the stress can be solved by measuring of resonant frequency. Currently, with the analysis of resonant spectral distribution, the vibration mode shapes identification is twinned.

Due to practical difficulties with the small membranes stress determination in bulging method the measurement of resonant frequencies has to be preferred.

Using the Laser Doppler Vibrometer (LDV)

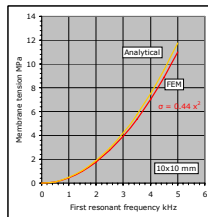
- point-wise mode of the periodic membrane deflections detection.
 - The observation of the membrane centre oscillations
 - many modal shapes are omitted
 - Vibrating membrane in atmosphere
 - adding mass of neighboring air must be taken into account.
- Mostly, the empirical expressions are used for such correction more or less successfully. Analyzing of a number of samples the average correction factors for the first natural mode have been determined:

Correction factors for air damping

$$f_{res}^{LDV} = 1.52 (10 \times 10 \text{ mm}^2)$$

$$f_{res}^{LDV} = 1.28 (5 \times 5 \text{ mm}^2)$$

$$f_{11} = \frac{\sqrt{2}}{2} \sqrt{\frac{S}{\gamma A}}$$



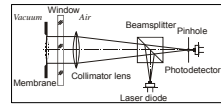
Nevertheless, these values have appeared **inaccurate and unreliable**. The measurement of vibrating membranes inside vacuum chamber through the glass window had to be arranged.

A number of specimens were analyzed.

- Tension stresses → **0 ÷ 30 MPa** - corresponding resonant frequencies up to **20 kHz**.
- Statistical assessment of the repeatability - measurement uncertainty - **Δσ = ± 0.1 MPa**

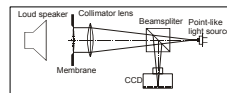
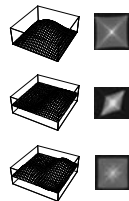
Vibrational measurement by confocal detector immediately inside the vacuum chamber.

- Detection of the changes in membrane surface sphericity



- long working distance mode of operation
- laser diode source 650 nm/5 mW
- objective lens 1:4, f = 105 mm
- pinhole opening diameter Φ = 0.1 mm
- photodiode detector OP 101

When using LDV the analysis of vibration spectra of membranes as a rule abounds in uncertainties of main resonant peaks identification
 ⇒ importance of the observation and visualization of modal shapes
 Based on the optical focal plane complex amplitude observation as well as phase visualization image to concept has been developed.



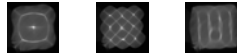
$$U(x_f, y_f) = \int_{-\infty}^{\infty} \int_{-\infty}^{\infty} \exp\left[i \frac{2\pi}{\lambda} w(x_0, y_0)\right] \exp\left[-i \frac{2\pi}{\lambda f} (x_0 x_f + y_0 y_f)\right] dx_0 dy_0$$

$$w(x_0, y_0) = A \sin(\Omega t) \sin\left(m \frac{\pi}{a} x_0 - \frac{\pi}{2}\right) \sin\left(n \frac{\pi}{a} y_0 - \frac{\pi}{2}\right)$$

$$m, n \in \mathbb{N}$$

$$\left(\frac{dw}{dx_0}\right)_{\max} = \frac{x_f \max}{2f} \quad A = w_{\max} = \frac{x_f \max a}{2\pi m f}$$

- Time-average intensity patterns at focal plane



- The examples of higher order modes obtained by time-averaged microscopic phase visualization

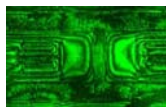
Both the methods make possible quantitative evaluation of membrane vibration amplitudes with the **nanometers sensitivity** for membrane deflections.

Dynamic/thermal behavior of membrane-like microcomponents

Determination of internal or residual stress in membrane microstructures have usually been realized either by observing the static shape residual deformation or the deformation forced to element. The membrane structure can also be excited to vibrate and to measure the natural frequency spectra.

Small dimensions of microcomponents - tens to hundreds of μm
 ⇒ limited conditions for tiny mechanical loading

- **Electrostatic excitation**
 - appropriate only for conductive layers
- **Thermal loading (mismatch of CTE-s)**
 - can influence properties of the structure
- **Laser impulse heating**
 - advantage in contactless excitation
- **Piezoelectric excitation**
 - excitation up to hundreds of kHz
- **Acoustic loading (acoustic pressure)**
 - limited range of frequencies 20 Hz ÷ 20 kHz

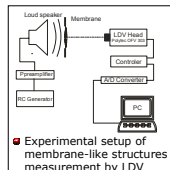


- Membrane structure of double cantilever

Acoustic pressure calibration

$$p = \rho c v \quad (\rho c)_{\text{air}} = 415 \text{ kg} \cdot \text{s}^{-1}$$

- loud speaker (60 ÷ 130 dB of the acoustic pressure)
- pistonphone chamber (173 Hz/118 dB - 15.8 Pa (RMS))



- Experimental setup of membrane-like structures measurement by LDV



Resonance frequencies characteristics of multilayer membrane systems

Cantilever beam

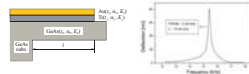


$$f = 0.162 \frac{h}{L^2} \sqrt{\frac{E}{\rho}}$$

Bridge

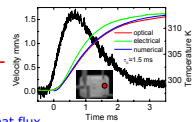


$$f = 1.03 \frac{h}{L^2} \sqrt{\frac{E}{\rho} \left(1 + \frac{3L^2 \sigma}{\pi^2 E k^2}\right)}$$



- Cantilever beam structure and its resonance curve. Damping factor $\epsilon = 4.5 \times 10^{-3}$

Laser Doppler vibrometer besides the vibrational measuring using also for **one-shot events detection**.



- 3D view of membrane microisland by confocal microscope

2D simulation of transient heat flux

$$k_{ef} \left(\frac{\partial^2 T}{\partial x^2} + \frac{\partial^2 T}{\partial y^2} \right) - \frac{h}{d} (T - T_0) - p_L + p_H = (\rho c)_d \frac{\partial T}{\partial t}$$

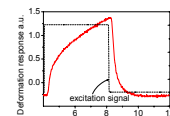
$$k_{ef} \left. \frac{\partial T}{\partial x} \right|_{x=0} = h(T - T_0) \Big|_{x=L=0}, \quad k_{ef} \left. \frac{\partial T}{\partial y} \right|_{y=0} = h(T - T_0) \Big|_{y=L}$$

$$k_{ef} = \frac{1}{d} \sum_i k_i d_i, \quad (\rho c)_d = \frac{1}{d} \sum_i \rho_i c_i d_i, \quad d = \sum_i d_i$$

Thermally induced deformation measurement
 T - temperature
 T₀ - ambient temperature
 k_{ef} - thermal conductivity coefficient
 (ρc)_d - volume specific heat
 h - heat transfer coefficient
 d - membrane structure thickness
 p_L - heat losses
 p_H - heat generation

Photothermal deflection spectroscopy (PDS)

- measuring of the sample deformation caused by optical absorption
- evaluating of layer material thermophysical parameters



Solution of heat conduction equation

$$T(r, t) = \frac{2P_0 \mu_0}{\pi c \rho r_0^2} \int_0^t \frac{1}{1 + 2t'/t_c} \exp\left(-\frac{2r^2}{t_c} / t_c'\right) dt'$$

$$t_c = \frac{r^2}{4\kappa}$$

- By monitoring of thermal parameters changes the microstructural modifications can be inspected.

Acknowledgement

This research has been supported in part by Austrian Federal Ministry of Science and Transport within the project No. GZ 603.505/2-V/B/9/99 in connection with the MEDEA project T611 for the development of Ion Projection Lithography for industrial applications and also by the NATO project SFP-974172 and VEGA project 9042/01.

References

- M. Drzik et al., "Optical Measurement of Stress in Thin Membranes", *Proc. of 26th IMEKO World Congress*, Ed. M.N. Durakbasa, Vienna, 2000.
- J. Butschke et al., "SOI Wafer Flow Process for Stencil Mask Fabrication", *Microelectronic Engineering* **46**, 1999, pp. 473-476.
- H. Loeschner et al., "Performance of Ion Projection Lithography (IPL)", *Proc. SEMI Technology Symposium 2001*, pp. 8/52-8/59.
- A. Heuberger, "Mikromechanik", *Springer-Verlag Berlin, Heidelberg, New York, London, Paris, Tokyo* 1989.
- B. A. Anderer and U. F. W. Behringer, "Determination of the Average Stress and Its Adjustment in the Silicon Membranes Used in Various Lithographies", *Microelectronic Engineering* **5**, 1986, pp. 67-71.
- A. Bosseboef, S. Petigand, "Characterization of the Static and Dynamic Behaviour of M(O)EMS by Optical Techniques: Status and Trends", *Proc. MME 02*, 2002, pp. 229-241.
- E. Sossna, A. Degen, I. W. Rangelow et al., "Mechanical Geometrical, and Electrical Characterization of Silicon Membranes for Open Stencil Masks", *J. Vac. Technol. B* **19**, 2001, pp. 2665-2670.
- P. Hrkut, M. Drzik et al., "The Influence of Ion Beam Bombardment on the Stress of Carbon Layers Prepared by RF Magnetron Sputtering", *Vacuum* **76**, 2004, pp. 329-333.
- P. Hudek et al., "Directly Sputtered Stress-compensated Carbon Protective Layer for Silicon Stencil Masks", *J. Vac. Sci. Technol. B* **17**(6), 1999, pp. 3127-3131.